

Effect of Microstructure Refinement on Magnetic Properties of Fe-Pt Thin Films

C. Y. Shen, F. T. Yuan

Abstract

$\text{Fe}_{53}\text{Pt}_{47}$ and $\text{Fe}_{58}\text{Pt}_{42}$ thin films with 300 nm in thickness prepared using magnetron sputtering were investigated. The films were deposited on heated glass substrates and annealed at 400°C and 800°C for different time. Single phase FePt films with similar chemical ordering but different substructure size were produced in the two series of samples. The effect of microstructure refinement results in significant enhancement in remanence (M_r) of about 38.1% and 30.8% in the $\text{Fe}_{53}\text{Pt}_{47}$ and $\text{Fe}_{58}\text{Pt}_{42}$ films, respectively. The energy product, $(BH)_{\text{max}}$, also showed a large increase of 25% and 72%; the maximum value of the two series of films are 16.2 MGOe and 19.6 MGOe, respectively. The large $(BH)_{\text{max}}$ was found to originate from the enhancement of M_r and steep slope of demagnetization curve at coercive point (α). As the theoretical predictions, in an isotropic magnet, the magnetic moments in the transition region of magnetization near grain boundary are easy to be aligned by applied field. In this study, it is found that by increasing the magnetic transition region through microstructure refining, the remanence can be effectively enhanced meanwhile facilitate the collective magnetic reversal. Domain structure confirms that the refinement of microstructure effectively reduces the domain size.

Keywords: FePt, microstructure refinement, energy product, exchange coupling, reversible magnetization.

微結構的細化對鐵鉑薄膜磁性質的效應

申繼陽、袁輔德

摘要

本研究針對厚度為 300 奈米的 $\text{Fe}_{53}\text{Pt}_{47}$ 和 $\text{Fe}_{58}\text{Pt}_{42}$ 兩種成分之薄膜進行一系列分析。薄膜試片以磁控濺鍍的方式沉積於加熱之玻璃基板上，加熱溫度為攝氏 400 和 800 度且持溫度不同時間。此製程可得到單相且具有相似序化度但不同微結構尺寸的鐵鉑薄膜。研究中發現微結構的細化明顯的增加了 $\text{Fe}_{53}\text{Pt}_{47}$ 和 $\text{Fe}_{58}\text{Pt}_{42}$ 試片的殘餘磁化量達 38.1%以及 30.8%。而磁能積亦分別增加了 25%以及 72%分別達到 16.2 以及 19.6MGOe。磁能積的增進除了起因於殘餘磁化量的增加外，亦與去磁曲線中較大的矯頑點斜率有關。在微磁學的理論預測中，在硬磁相邊界處的磁矩由於靜磁能作用的緣故而較不穩定因而易被外加磁場磁化；於本實驗中則證實了藉由細化微結構而導致的磁性不穩定區域的增加，可有效的增進薄膜的殘餘磁化量同時促進整合性的磁化反轉。

關鍵詞：鐵鉑、微結構細化、磁能積、交互耦合、可逆磁化。

I. INTRODUCTION

ORDERED EQUI-ATOMIC FePt phase with a structure of face-centered tetragonal (fct) is of interest in areas such as magnetic recording and permanent magnet owing to its very high anisotropy (K_u) and Curie temperature. Comparing to other high performance magnet like Sm-Co and Re-Fe-B (Re: rare earth element), FePt also shows excellent chemical stability which makes it becomes a potential candidate for bio-used magnet. However, its magnetic performance, usually indexed by energy product $[(BH)_{\max}]$, is much lower than that of currently used Sm-Co or Re-Fe-B. Generally, based on the theoretical studies [1]-[3], the magnetic performance of a magnet can be largely improved by introducing a soft magnetic phase and controlling microstructure. The strong exchange coupling between high coercivity hard phase and high magnetization soft phase increases the $(BH)_{\max}$ of the whole magnet. Many efforts have been focused on this goal to introduce soft magnetic phase in FePt $L1_0$ matrix [4]-[8]. A very high value of $(BH)_{\max}$ of larger than 40 MGOe has been achieved in a nanostructured FePt-Fe₃Pt film exhibiting exchange-spring behavior prepared by multilayer deposition with ~60 nm in

thickness [4]. Enhancements in $(BH)_{\max}$ though exchange coupling have also been reported in FePt/Fe bilayer thin films [7] and Fe-Pt-B melt-spinning ribbons [8].

Apart from the nanocomposite two-phase magnets, the refinement of grain size in a isotropic single phase hard magnetic material can also enhance the $(BH)_{\max}$ as predicted by micromagnetic simulation by Schrefl *et al.* [2]. The physical origin is explained by the remanence enhancement resulted from the unstable moment near the grain boundaries. Experimental study on single phase Nd-Fe-B [9] and two-phase [10] Nd-Fe-B+ α Fe agrees well with the theoretical predictions. Unlike the intermetallic Re-Fe-B possesses an invariable stoichiometry of 2:14:1, the composition of $L1_0$ FePt displays a wide range, resulting in a broad anisotropy distribution in a single phase sample, which is not considered in the Schrefl's work [2]. We therefore expected that the size dependence of magnetic properties in $L1_0$ FePt can be much different from Re-Fe-B system. However, very few works concerning this issue have been reported. In this study, the focus was placed on the relation between microstructure refinement and magnetic properties in single phase Fe-Pt films.

II. EXPERIMENTAL

Thin film samples were deposited by radio frequency (rf) magnetron sputtering under a background vacuum better than 2×10^{-7} torr. The sputter deposition is performed in argon atmosphere with 10 mtorr in pressure. A composite target consisting of an iron disk overlaying with Pt foils was used. The composition of the deposited films was controlled by adjusting the size of Pt foils. Single layer films with thickness of 300 nm were deposited on heating Corning 1737 glass substrate at 400 and 800°C. After the deposition, the substrate temperature (T_a) was maintained for different time (t): 400°C for 10, 30, 60, 150, 600, and 900 minutes, and 800°C for 60 minutes to create single phase (homogeneous) structure and control the grain size. Two compositions of the FePt films were prepared for comparison: Fe₅₃Pt₄₇ and Fe₅₈Pt₄₂, which were confirmed by inductive coupled plasma (ICP) technique. Structural analysis was carried out using a rotated anode X-ray diffractometer. In-plane magnetic properties were measured at room temperature using a vibrating sample magnetometer (VSM) with maximum applied field of 2 T. Microstructure was studied by using transmission electron microscope (TEM).

III. STRUCTURAL RESULTS

Fig. 1 shows the XRD patterns for the Fe₅₃Pt₄₇ sample deposited at 400°C with $t = 10, 30$ min, and 15 hours, and Fe₅₈Pt₄₂ sample for 15 hours, respectively. The patterns exhibit narrow and sharp superlattice peaks of (001), (110), the splitted {200}, and (103), indicating an isotropic Ll_0 phase of FePt. Order parameter (S_{order}) representing the extent of ordering in the Ll_0 phase was measured using the method described in [11]. The diffraction peaks of (001) and (002) were taken as superlattice and fundamental peaks to obtain order parameter, which allow us to confine the obtained results to the ordered region rather than the whole sample. The raw value of S_{order} (S_r) measured from the integrated intensities of the chosen peaks needs further modification for the deviation of equi-atomic composition of FePt [12]. The real order parameter, S_{order} , equal to $(S_r - 2\Delta x)$; where Δx represents the compositional deviation in atomic percentage. The obtained S_{order} can be an underestimated value, because the richness of Fe reduces S_r . The values of S_{order} were listed beside each pattern in Fig. 1, which indicates that the chemical ordering of Fe₅₃Pt₄₇ films shows no further enhancing while the annealing time longer than 30 minutes at 400°C.

FIGURE 1 HERE

Apart from the S_{order} , the chemical ordering can be monitored more detailed by another index of volume fraction (f_0) of order phase [12]. This index is especially important for this study, because of order and disorder phase of FePt possess different magnetism (hard and soft magnetic), and the distribution of which determines the magnetic properties. Slow scan profile of {200} and {220} group can be used to measure f_0 the detailed method is described in [12]. Fig. 2 shows the profiles for the $\text{Fe}_{53}\text{Pt}_{47}$ film annealed at 400°C with $t = 10$ and 30 min and the $\text{Fe}_{58}\text{Pt}_{42}$ film for 15 hours. The profiles can be perfectly fitted by Lorenzan fitting into (220) and (202) peaks indexing the $L1_0$ structure; no peak belongs to the disordered $A1$ phase between the two separated ones were observed, that is, $f_0 \sim 1$. This confirms that the films are structural homogeneous of $L1_0$ phase even for the sample with $t=10$ min deposited at 400°C .

FIGURE 2 HERE

Mean substructure size, the size of a region separated by various kinds of planar defects including stacking faults, dislocation walls, twin, anti-phase, and grain boundaries, etc., of the samples was studied. Stoke-Wilson method [13] was adopted in this paper rather

than Scherrer method due to which is developed for thin film samples containing certain internal strain or stress. Fig. 3 shows the relation between Stoke-Wilson size (D_{SW}) and t for the films with different composition. It indicates that in the $\text{Fe}_{53}\text{Pt}_{47}$ films with $T_a = 400^\circ\text{C}$, the D_{SW} increased from 26 nm to 48 nm while t was increased from 10 min to 15 hours. As T_a was increased to 800°C , a large D_{SW} of about 55 nm was obtained. In the $\text{Fe}_{58}\text{Pt}_{42}$ films, the D_{SW} is much smaller than that of the $\text{Fe}_{53}\text{Pt}_{47}$ samples even at high T_a of 800°C (~ 29 nm). The measured order domain size in this paper is larger than that observed in [14] for FePt bulk alloy.

FIGURE 3 HERE**IV. Magnetic Properties**

Fig. 4 illustrates the hysteresis loops for the $\text{Fe}_{53}\text{Pt}_{47}$ films with $T_a = 400^\circ\text{C}$ and 800°C ; $t = 10$ min and 1 hour, respectively. Both films are magnetically single phase. The sample with $T_a = 400^\circ\text{C}$ showed high magnetization at applied field of 2T ($M_{2\text{T}}$) of 970 emu/cm³ and remanence (M_r) of 740 emu/cm³; for $T_a = 800^\circ\text{C}$ film, $M_{2\text{T}}$ decreased to 700 emu/cm³ and M_r to 535 emu/cm³; but the coercivity (H_c) was similar (~ 6.5 kOe). The virgin curve of the two films exhibits

different initial slope, which suggests that the reversal process is dominated by different mechanisms: domain wall pinning for the 400°C annealed film with a smaller initial slope; rotation for the 800°C one with a steeper slope.

FIGURE 4 HERE

Magnetic properties including M_r , H_c , $(BH)_{\max}$, and the slope of demagnetization curve at coercive point in a hysteresis loop (α) for the $\text{Fe}_{53}\text{Pt}_{47}$ and $\text{Fe}_{58}\text{Pt}_{42}$ films with different annealing condition are shown in Fig. 5(a)-5(d), respectively. It was indicated that in the $\text{Fe}_{53}\text{Pt}_{47}$ films with $T_a = 400^\circ\text{C}$, M_r continuously decreased from 740 emu/cm^3 to 631 emu/cm^3 . A highest M_r of 883 emu/cm^3 was obtained in the Fe-rich film annealed at 400°C. For the 800°C-annealed samples of $\text{Fe}_{53}\text{Pt}_{47}$ and $\text{Fe}_{58}\text{Pt}_{42}$, M_r equal to 535 emu/cm^3 and 675 emu/cm^3 , respectively. Comparing to the structural results, the decrement of M_r can be related to the enhanced chemical ordering. H_c for the two series of films appears to be independent with T_a and t , values about 6.5 kOe were shown except for the $\text{Fe}_{58}\text{Pt}_{42}$ films with $T_a = 800^\circ\text{C}$ (4.7 kOe). The slope α , defined as $4\pi(dM/dH)_{H_c}$, were used to illustrate the reversal coherency of a demagnetizing

process: large α demonstrates a cooperative reversal, and the small value represents discontinuous demagnetizing. Several factors can determine α of a thin film, including microstructure, magnetic homogeneity (anisotropy distribution), exchange interactions, etc. In this study, the samples exhibit magnetic and structural single phase and continuous microstructure; α thus mainly influenced by size (D_{SW}) and composition. Fig. 5(c) shows the relation between α and t . It indicates that the enrichment of iron and the low temperature annealing results in large α . Dependence of $(BH)_{\max}$ on t was illustrated in Fig. 5(d). In the $\text{Fe}_{53}\text{Pt}_{47}$ films annealed at 400°C, $(BH)_{\max}$ decreased by ~19% to 13 MGOe with the increasing of t . The maximum $(BH)_{\max}$ of 19.6 MGOe was obtained in the iron-rich sample with $T_a = 400^\circ\text{C}$. The presented results clearly show that the $(BH)_{\max}$ is mainly determined by M_r and α .

FIGURE 5 HERE

V. Discussion

The present results showed a significant enhancement in energy product in the low-temperature annealed iron-rich single phase FePt film. This enhancement is found to be

determined by high M_r and α as illustrated in Fig. 5. As described by Schrefl *et al.*, magnetization enhancement in an isotropic single phase magnet is originated from the moment near grain boundaries [2]. Due to the large angle between the easy-axis of the adjacent grains, the alignment of magnetization near the boundary region deviates from the center of grain. These unstable moments are easy to be aligned by applied field. As the grain size is reduced, the unstable region increases, resulting in a significant remanence enhancement. This mechanism can be a reasonable explanation for the M_r improvement obtained in the two series of FePt films. Additionally, the presented data indicates that the enrichment of Fe can further increase M_r without sacrificing coercivity.

The enhancement in remanence by microstructure refinement reached 38.1% and 30.8% for the Fe₅₃Pt₄₇ and Fe₅₈Pt₄₂ sample, respectively; which is significantly larger than the results obtained by Manaf *et al.* in Nd-Fe-B ribbon (18%). Reasons for this obvious discrepancy are suggested as follows.

1. Composition inhomogeneous: unlike Nd₂Fe₁₄B as an intermetallic compound with a fixed stoichiometry; FePt L_{10} phase exists within a wide range of composition, that is, a

compositional distribution appears in grains of a film. This enlarges the anisotropy distribution, which may increase M_r by enhancing exchange coupling between FePt grains.

2. Boundary disordering: as reported by Takahashi *et al.*, the chemical ordering of FePt L_{10} phase decrease near phase surface [15], which degrades anisotropy and results in further increase of M_r .

REFERENCES

- [1]E. F. Kneller and R. Hawig "The exchange-spring magnet: A new material principle for permanent magnets," *IEEE Trans. Magn.*, vol. 27, pp. 3588-3600, 1991.
- [2]T. Schrefl, J. Fidler, and H. Kronmuller, "Remanence and coercivity in isotropic nanocrystalline permanent magnets," *Phys. Rev. B*, vol. 49, pp. 6100-6110, 1994.
- [3]H. Kronmuller, R. Fischer, M. Seeger, and A. Zern, "Micromagnetism and microstructure of hard magnetic materials," *J. Phys. D*, vol. 29, pp. 2274-2283, 1996.
- [4]J. P. Liu, C. P. Luo, Y. Liu, and D. J. Sellmyer, "High energy products in rapidly annealed nanoscale Fe/Pt multilayers,"

- Appl. Phys. Lett.*, vol. 72, pp. 483-485, 1998.
- [5] J. Zhou, Ralph. Skomski, X. Li, W. Tang, G. C. Hadjipanayis, and D. J. Sellmyer, "Permanent-magnet properties of thermally processed FePt and FePt-Fe multilayer films," *IEEE Trans. Magn.*, vol. 38, pp. 2802-2804, 2002.
- [6] P. D. Thang, E. Bruck, F. D. Tichelaar, K. H. J. Buschow, and F. R. de Boer, "Magnetic properties and microstructure of Fe-Pt-based alloys," *IEEE Trans. Magn.*, vol. 38, pp. 2934-2936, 2002.
- [7] Y. K. Takahashi, T. O. Seki, K. Hono, T. Shima, and K. Takahashi, *J. Appl. Phys.*, vol. 96, pp. 475-481, 2004.
- [8] W. Zhang, D. V. Louzguine, and A. Inoue, "Synthesis and magnetic properties of Fe-Pt-B nanocomposite permanent magnets with low Pt concentrations," *Appl. Phys. Lett.*, vol. 85, pp. 4998-5000, 2004.
- [9] A. Manaf, R. A. Buckley, H. A. Davies, and M. Leonowicz, "Enhanced Magnetic Properties in Rapidly Solidified Nd-Fe-B Based Alloys," *J. Magn. Mater.*, vol. 101, pp. 360-362, 1991.
- [10] O. V. Billoni, S. E. Urreta, L. M. Fabietti, and H. R. Bertorello, "Dependence of the coercivity on the grain size in the FeNdB+ α Fe nanocrystalline composite with enhanced remanence," *J. Magn. Mater.*, vol. 187, pp. 371-380, 1998.
- [11] B. E. Warren, *X-Ray Diffraction* (Addison-Wesley, Reading, MA, 1969).
- [12] A. Cebollada, R. F. C. Farrow, and M. F. Toney, in *Magnetic Nanostructures*, edited by H. S. Nalwa (American Scientific, Stevenson Ranch, CA, 2002), p. 93.
- [13] A. J. C. Wilson, *X-Ray Optics* (Methuen, London, 1949), p. 33.
- [14] Y. Tanaka and K. Hisatsune, "Remanence enhancement based on Ll_0 ordering in Fe-Pt permanent magnets," *J. Appl. Phys.*, vol. 93, pp. 3435-3439, 2003.
- [15] Y. K. Takahashi, T. Koyama, M. Ohnuma, T. Ohkubo, and K. Hono, "Size dependence of ordering in FePt nanoparticles," *J. Appl. Phys.*, vol. 95, pp. 2690-2696, 2004.
-

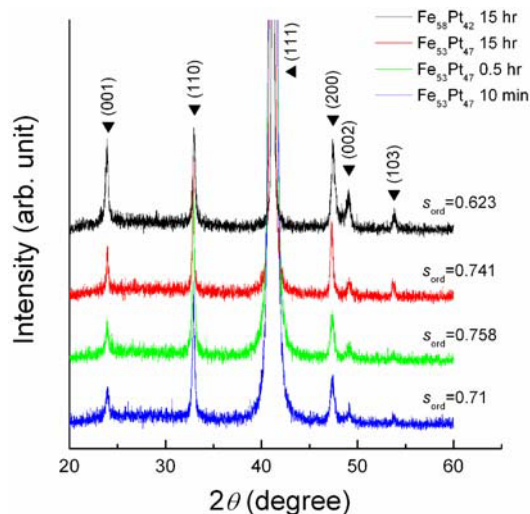


Fig. 1. XRD patterns for the samples of $\text{Fe}_{53}\text{Pt}_{47}$ and $\text{Fe}_{58}\text{Pt}_{42}$ annealed at 400°C for different time.

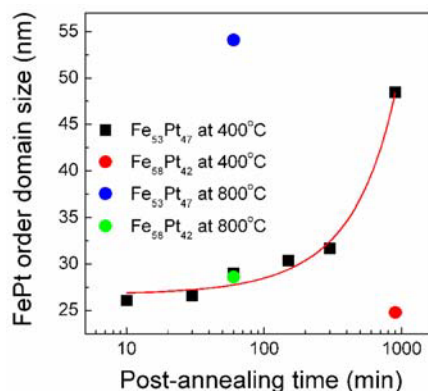


Fig. 3. Dependence of order domain size on post-annealing time for the sample of $\text{Fe}_{53}\text{Pt}_{47}$ and $\text{Fe}_{58}\text{Pt}_{42}$ deposited at 400°C and 800°C , respectively.

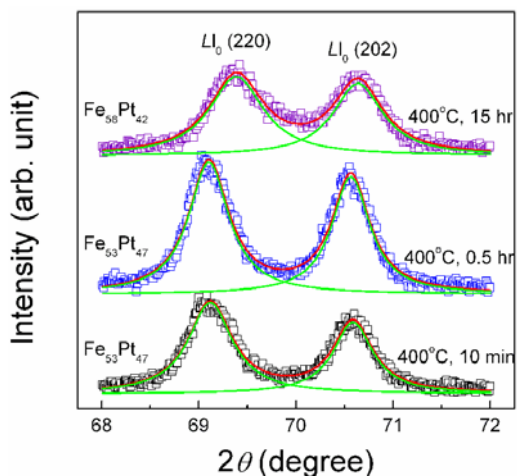


Fig. 2. XRD slow scan patterns for the samples of $\text{Fe}_{53}\text{Pt}_{47}$ and $\text{Fe}_{58}\text{Pt}_{42}$ annealed at 400°C for different time.

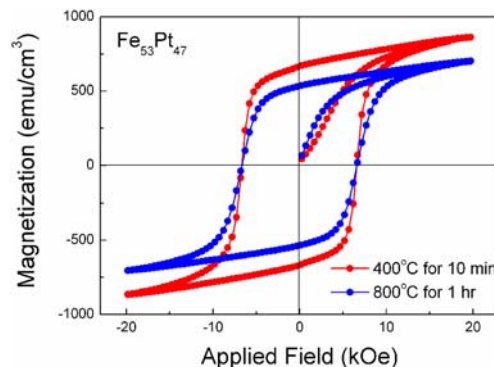


Fig. 4. Hysteresis loops for the $\text{Fe}_{58}\text{Pt}_{42}$ samples annealed at 400°C and 800°C .

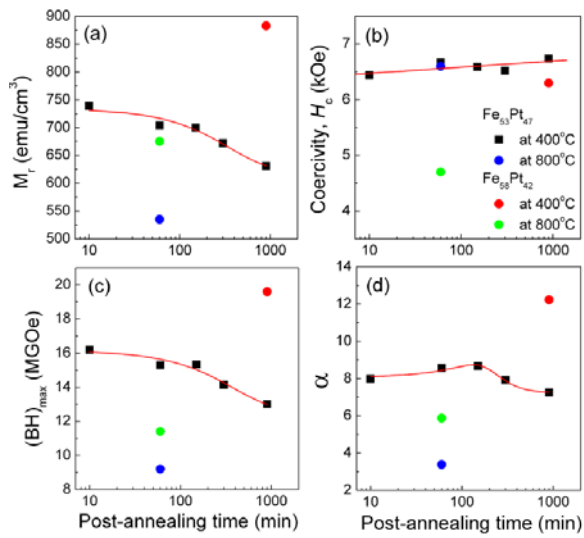


Fig. 5. Dependence of (a) remanence, M_r ; (b) coercivity, H_c ; (c) slope of demagnetizing curve at coercive point; and (d) energy product $(BH)_{\max}$ on post-annealing time for the $\text{Fe}_{53}\text{Pt}_{47}$ and $\text{Fe}_{58}\text{Pt}_{42}$ samples deposited at different temperature.